J. Chem. Soc. Nigeria, Vol. 48, No. 5, pp 1001 - 1014 [2023] https://doi.org/10.46602/jcsn.v48i5.928

STRUCTURAL INVESTIGATION OF HETERO-STRUCTURED CORE-SHELL SILVER-SILICA HYBRID AS A POTENTIAL AGRO-SENSOR MATERIAL

F. O. Oladoyinbo[1], F. O. Sanni[1,5], F. Akinwunmi[1], K. A. Amusa[2], S. A. Ganiyu[3], W. B. Ayinde[4,6], J. A. Aremu[1], Q. O. Yusuf[7], A. K. Akinlabi[1], E. O. Dare[1]

1 Department of Chemistry, College of Physical Sciences, Federal University of Agriculture Abeokuta, PMB 2240, Alabata Road, Abeokuta, Nigeria

2. Department of Electrical Engineering, College of Engineering, Federal University of Agriculture Abeokuta, PMB 2240, Alabata Road, Abeokuta, Nigeria

3. Department of Physics, College of Physical Sciences, Federal University of Agriculture Abeokuta, PMB 2240, Alabata Road, Abeokuta, Nigeria

4. Environmental Remediation and Nanoscience, Department of Geography and Environmental Sciences, Faculty of Agriculture, Science and Engineering, University of Venda, Thohoyandou, South Africa.

5. Research and Development Department, FESCOSOF Data Solution, Ogun State, Nigeria.

6. Water Research Group & ASPECT, Department of Civil Engineering, Faculty of Engineering and Built Environment, Upper Campus, University of Cape Town. South Africa.

7. Department of Microbiology, College of Biological Sciences, Federal University of Agriculture Abeokuta, PMB 2240, Alabata Road, Abeokuta, Nigeria

ABSTRACT

Investigation into the novel synthesis and structural properties of Heterostructured core shell Silver-Silica ($AgSiO_2$) Nanohybrid is reported herein, for possible utilization as humidity sensing material in Agricultural post-harvest humidity monitoring system and greenhouse farming. The Heterostructured nanoparticles (Ag and SiO_2) were synthesized via a chemical reduction method. Structural characterizations were done using X-ray Diffraction (XRD), High Resolution Transmission Electron Microscopy (HRTEM), Scanning Electron Microscopy (SEM), UV-Visible spectroscopy, Energy Dispersive X-ray (EDX) spectroscopy and N_2 adsorption-desorption techniques. The XRD diffractogram of Ag-SiO_2 showed distinct peaks at 2θ values of 39^0, 43^0, 66^0 and 79^0 which was corroborated by the SEM and HRTEM results. EDX convincingly confirmed Ag and SiO_2 incorporation into the Ag-SiO_2 nanocomposite hetero-structure at 16.7 % and 83.3 % respectively. A Surface Plasmon Resonance absorption peak of 421 nm of Ag was revealed by UV-Visible spectroscopic analysis. An effective and relatively narrow pore size distributions of 3 – 8 nm was revealed by N_2 adsorption-desorption for the Ag-SiO_2 Nanocomposite. Overall, these properties are promising for effective use as humidity sensing material.

Key words: Silver, Silica, Nanocomposite, Nanohybrid,

INTRODUCTION

Nanocomposites are composites in which at least one of the phases shows dimensions in the nanometre range (1 nm = 10^{-9} m)[1]. Nanocomposite materials have emerged as suitable alternatives to overcome limitations of micro-composites and monolithics, while posing preparation challenges related to the control of elemental composition and stoichiometry in the nanocluster phase. They are reported to be the materials of 21st century in the view of possessing design uniqueness and property combinations that are not found in conventional composites. The general understanding of these properties is yet to be reached [2], even though the first inference on

ISSN 0795 - 22066

them was reported by Gleiter in 1992 [3]. It has been reported that changes in particle properties can be observed when the particle size is less than a particular level, called 'the critical size'[4]. Additionally, as dimensions reach the nanometre level, interactions at phase interfaces become largely improved, and this is important to enhance materials properties.

Prospects in nanocomposites

Ceramics have good wear resistance and high thermal and chemical stability. However, they are brittle. In this context, the low toughness of ceramics has remained a stumbling block for their wider use in industry. In order to overcome this limitation, ceramic-matrix nanocomposites have been receiving attention, primarily due to the significant enhancement on mechanical properties which can be achieved. For example, the incorporation of energy-dissipating components such as whiskers, fibres, platelets or particles in the ceramic matrix may lead to increased fracture toughness [5][6]. Metal matrix nanocomposites (MMNC) refer to materials consisting of a ductile metal or alloy matrix in which some nanosized reinforcement material is implanted. These materials combine metal and ceramic features: ductility and toughness with high strength and modulus. Thus, metal matrix nanocomposites are suitable for production of materials with high strength in shear/compression processes and high service temperature capabilities. They show an extraordinary potential for application in many areas, such as aerospace and automotive industries and development of structural materials [7]. Polymer materials are widely used in industry due to their ease of production, lightweight and often ductile nature. However, they have some disadvantages such as low modulus and strength compared to metals and ceramics. In this context, a very effective approach to improve mechanical properties is to add fibres, whiskers, platelets or particles as reinforcements to the polymer matrix. Polymers have been filled with several inorganic compounds, either synthetic or natural, in order to increase heat and impact resistance, flame retardancy and mechanical strength, and to decrease electrical conductivity and gas permeability with respect to oxygen and water vapour [8].

Methods for the synthesis of nanoparticles

Metallic nanoparticles may be synthesized by a variety of methods, which can produce particles of multiple morphologies for a diverse range of applications [9]. The major reported route is the production of colloidal dispersions using chemical – reduction method, a well-established method [10]. The method involves the reduction of metals by chemical means and is very popular due to the relative ease of production of nanomaterials. The advantages of this process include: mild reaction conditions, low energy consumption and simple separation procedures with high yields and relatively short reaction times [11]. General methods of colloid synthesis like the Lee – Meisel method are uncomplicated and hence popular modes of producing silver colloids [12]. In such processes, solutes are initially formed to yield a supersaturated solution, leading to nucleation. The formed nuclei may further grow by a diffusive mechanism. The resulting primary particles

ISSN 0795 - 22066

aggregate to form secondary particles. This latter process is sometimes facilitated by changes in the chemical conditions in the system: the ionic strength may increase, or the pH may change, causing the surface potential to approach the isoelectric point. Formation of the final (secondary) particles of narrow size distribution is a diffusion-controlled aggregation process, proceeding via the addition-polymerization type growth by irreversible capture of primary particle aggregates [13]. The final morphology of the nanoparticles is mostly determined by experimental conditions such as; the reducing and stabilizing agents [14].

It follows that adjustments to the fabrication technique can give significant changes to the nanoparticles morphology, for example using citrate as the reducing agent requires additional energy (increased temperature) to produce a colloid whereas sodium borohydride readily reduces the silver ions in a solution. This is also true for the choice and concentration of stabilizing agent used for smaller particles that are obtained by increasing the stabilizer concentration [15]. More over as the potential applications of metallic nanoparticles continue to increase, current industrial needs demand quicker, simpler, more cost effective, robust and reliable means of nanomaterial production. The demand for customized nanostructures is application driven; due to the novel features exhibited by silver nanomaterials that are dictated by the particle's structure.

Importance of silver and Silica nanoparticles

Silver is one of the basic elements that make up our planet. It is a rare, but naturally occurring element, slightly harder than gold and very ductile and malleable. Pure silver has the highest electrical and thermal conductivity of all metals and has the lowest contact resistance. Silver can be present in four different oxidation states: Ag^0, Ag^+, Ag^{2+}, Ag^{3+}. The former two are the most abundant ones while the latter are unstable in the aquatic environment. [16]. Metallic silver itself is insoluble in water, but metallic salts such as $AgNO_3$ and Silver chloride are soluble in water[17]. Metallic silver is used for the surgical prosthesis and splints, fungicides and coinage. Soluble silver compounds such as silver salts have been used in treating mental illness, epilepsy, nicotine addition, gastroenteritis and infectious diseases including syphilis and gonorrhea [18]. Metallic silver appears to pose minimal risk to health, whereas soluble silver compounds are more readily absorbed and have the potential to produce adverse effects [9][18]. The wide variety of uses of silver allows exposure through various routes of entry into the body. Ingestion is the primary route for entry for silver compounds and colloidal silver proteins. Dietary intake of silver is estimated at 70-90 μg/day. Since silver in any form is not thought to be toxic to the immune, cardiovascular, nervous or reproductive system and it is not considered to be carcinogenic, silver is relatively non-toxic [19][20]. Silver demand will likely rise as silver find new uses, particularly in textiles, plastics and medical industries, changing the pattern of silver emission as these technologies and products diffuse through the global economy[21].

Silicon is the second most common element in earth's crust and comes in many forms. The metalloid nature of Si allows this tetravalent

ISSN 0795 - 22066

element to readily bond to the degree that pure silicon is relatively rare. Silicon is frequently bonded to oxygen, the most common of the elements in earth's crust, in the form of silicon oxides. In general, silicon oxide forms with four oxygen atoms surrounding each silicon atom forming large interconnected networks. This material has the formula SiO_2 and is known as silicon dioxide or silica and is able to form many different structures both crystalline and amorphous such as quartz and glass respectively. In addition, silica structures can really incorporate into other elements such as aluminum and silver. Silica is also able to form a variety of porous structures in crystalline and amorphous forms. These silica based porous materials are well studied and used due to their variable properties high abundance [22]. Silicon dioxide nanoparticles, also known as silica nanoparticles or nanosilica, are the basis for a great deal of biomedical research due to their stability, low toxicity and ability to be functionalized with a range of molecules and polymers. Nano-silica particles are divided into P-type and S-type according to their structure. The P-type particles are characterized by numerous nanopores having a pore rate of 0.61 mL/g. The S-type particles have a comparatively smaller surface area. The P-type nano-silica particles exhibit a higher ultraviolet reflectivity when compared to the S-type. Silica nanoparticles appear in the form of a white powder with density of 2.4 g/cm^3 and molar mass of 59.96 g/mol. Silica nanoparticle is used as additive for rubber and plastics, strengthening filler for concrete and other construction composites as well as a stable, non-toxic platform for biomedical applications such as drug delivery and theragnostic [23][17].

MATERIALS AND METHODS

Materials

Silver nitrate, Ascorbic Acid, Tri-sodium citrate (TSC), Hydrochloric acid and Sodium silicate were all purchased from Sigma Aldrich and used as received without further purification. Characterization of silver nanoparticle, silica and silver-silica nanocomposite were done, using both atomic and scanning devices which included: XRD – X-ray Diffraction crystallography, Nitrogen adsorption-desorption Isotherm, XPS – X-ray Photoelectron Spectroscopy, TEM - Transmission Electron Microscopy and UV-Visible Spectroscopy.

Synthesis of silver nanoparticles

In the nanocomposite preparation, the silver nanoparticles were synthesized by chemical reduction of silver nitrate ($AgNO_3$) with ascorbic acid ($C_6H_8O_6$) in an aqueous medium with tri-sodium citrate (stabilizing) agent. The role of tri-sodium citrate as a capping agent is well-documented by [24], and it was observed that, in this case, without the presence of the stabilizer, the stability of the colloids was drastically reduced with metallic silver formed due to aggregation of nanoparticles. Silver nanoparticles were obtained by dissolving 0.85 g of $AgNO_3$ in 5ml distilled water and stirring for about 20 min at 120 ^oC. To this, sodium citrate solution (0.5 g) was added. Ascorbic acid solution (1.4 g) was added drop wise to the above solution and stirred until colloidal

ISSN 0795 - 22066

particles of silver formed. A colour transition from light yellow to light brown is an evidence of nucleation and growth of silver nanoparticles. Sodium citrate was used as a stabilizing or capping agent to prevent the aggregation of nanoparticles and to control the size of the nanoparticles, while ascorbic acid was used as a reducing agent.

$$4AgNO_3 + C_6H_7O_5Na_3\,H_2O \longrightarrow 4Ag^0 + C_6H_5O_2H_3 + 3Na^+ + 3H^+ + 2O_2$$

Synthesis of silica nanoparticles

Silica was synthesized following the method of [25]. Under vigorous stirring, 1.0 g of Cetyl Trimethylammonium Bromide (CTAB) was added to 10 mL hydrochloric (HCl) acid and heated at 80 ^oC until a clear solution was formed. 20 mL of distilled water was added to the mixture and stirred for 15 minutes after which 10 mL of Sodium silicate was added and stirred for another 30 minutes. The solution was allowed to age for 30 minutes and then filtered to retrieve the silica.

Synthesis of silver–silica nanocomposite

Silver and silica nanoparticles were synthesized as described previously in sections 3.2.1 and 3.2.2. 0.6 g of synthesized silica was added to the silver and stirred for 30 min at 70 ^oC. The mixture was centrifuged at 4400 rpm for 10 min at room temperature. A brown-coloured precipitate with supernatant was formed. The supernatant was decanted and the Ag – SiO_2 nanocomposite was dried at 100 ^oC for 2 hours (Figure 1).

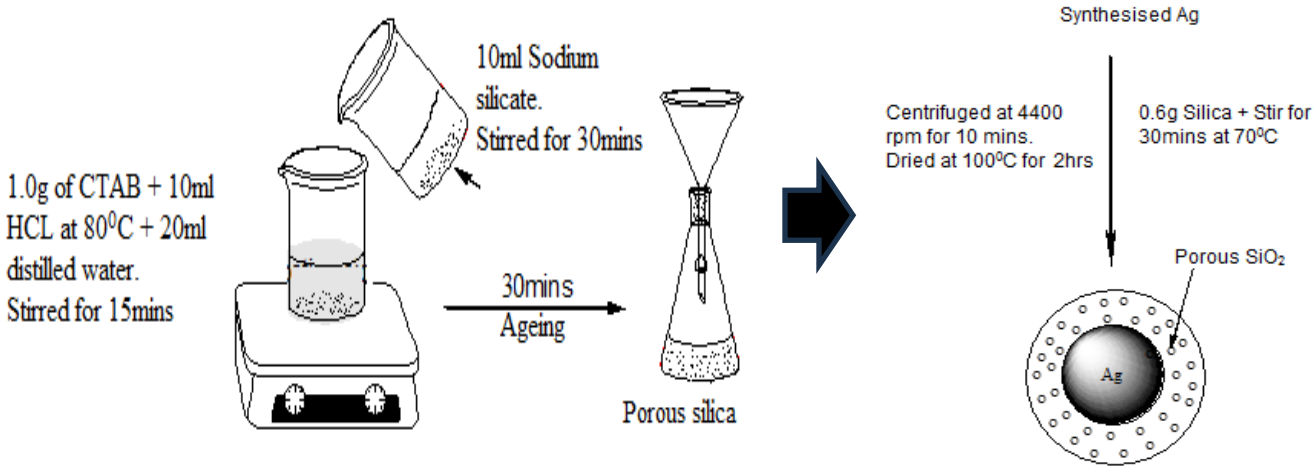

Figure 1: Synthesis of porous silica and Ag-SiO_2 nanocomposite

Characterization of silver, silica nanoparticles and silver-silica nanocomposite

UV-Vis analysis

In silica nanoparticles the optical phenomena is related to the presence of different defects due to incomplete formation of Si – O - Si tetrahedral network at the silica surface, such as oxygen and silicon vacancies [26][27]. To study the effect of particles size on electronic absorption behavior, UV – Vis diffuse-reflectance absorption spectra were recorded on a Shimadzu UV – 2401 PC spectrophotometer. The spectra were taken in different time intervals up to 24 hours between 350 nm to 500 nm.

ISSN 0795 - 22066

X-Ray Diffraction (XRD) analysis

The phase variety and grain size of synthesized silver, silica nanoparticles and Ag-SiO_2 nanocomposite were determined by X-ray diffraction spectroscopy (Philips PAN analytical). The synthesized nanoparticles and nanocomposite were studies with Cu-Kα radiation at voltage of 30 kV and current of 20 MA with scan rate of 0.03 ^{0}/s, λ = 1.54 Å

SEM analysis

The morphological features of synthesized nanoparticles and nanocomposites were studied by NOVA Nano - Scanning Electron Microscope (JSM - 6480 LV). The SEM slides were prepared by making a smear of the solutions on slides. A thin layer of platinum was coated to make the samples conductive. Then the samples were characterized in the SEM at an accelerating voltage of 5 - 20 KeV, emission current of 75 – 80 A and working distance of 6 – 13 nm.

XPS analysis

An X-ray photoelectron spectrometer (XPS) was used to characterize the chemical composition and chemical bonds. The XPS spectra were fitted by XPS peak software, and Shirley background was chosen for background calculation of the XPS spectra.

Pore size and pore distribution

Nitrogen adsorption/desorption isotherms were measured at the liquid nitrogen temperature using a Nova 1000 analyzer. Specific surface areas were calculated using the BET method. Pore size distributions were evaluated using BJH method.

RESULTS AND DISCUSSION

Results of X-ray Diffraction Spectroscopy

Figure 3 shows an X-ray diffraction pattern of silica. A broad band with Bragg's angle at 2θ = 22°, which is the characteristic band of amorphous silica walls of the pristine material was observed. The result obtained corresponds to the observed result for mesoporous silica in a similar work of by Tomer *et al* [28][29] though the Ag-loaded mesoporous silica SBA-15 nanocomposites were prepared via hydrothermal process while the current research involved formation of heterostructured core-shell Ag-SiO_2 nanohybrid by chemical reduction method. The presence of amorphous silica was confirmed due to absence of peak near Bragg's 2θ of 26˚, which confirms the absence of crystoballite nanoparticles [30]. X-ray diffraction (XRD) micrograph of Ag nanoparticles showed a number of strong Bragg's reflections which correspond to the (111, ~ 39^0), (200, ~ 45^0), (220, ~ 66^0) and (311, ~ 79^0) reflections of face centred cubic silver (Figure 4). This is an indication that the silver nanoparticles within the coating were crystalline. A similar finding was reported by Anandalakshmi *et al* [31] and Jyoti *et al* [32] who identified peaks at (2θ) 38.19, 44.37, 64.56 and 77.47 corresponding to the (111), (200), (220) and (311) planes respectively. The average crystalline size was calculated using Debye - Scherrer formula,

$$D = \frac{0.9\lambda}{\beta cos\theta}$$

Where D is the average crystalline size of the nanoparticles, 0.9 is geometric factor (k), λ is the wavelength of X-ray radiation source (0.15406 nm) and β is the angular full-width at half maximum

ISSN 0795 - 22066

(FWHM = 0.004) of the XRD peak at the diffraction angle θ [33]. The calculated average crystallite of the silver nanoparticles (AgNPs) is ~37 nm is higher than ~25 nm obtained by Jyoti *et al* [22].

Figure 5 shows the X-ray diffraction pattern for Ag-SiO_2, the broad diffraction peaks showed that the samples contained very small particles. The major peaks of Ag powder were observed at 2θ values of 39^0, 43^0, 66^0 and 79^0 respectively. These sharp Bragg's peaks correspond to the peaks of pure silver (Figure 3) and might have resulted due to capping agent stabilizing the nanoparticles. Intense Bragg's reflections suggest strong X-ray scattering centres in the crystalline phase and could be due to capping agents. Generally, the broadening of peaks in the XRD patterns of solids is attributed to particle size effects. Broader peaks signify smaller particle sizes and reflect the effects due to experimental conditions on the nucleation and growth of the crystal nuclei[34]. The spectrum of silica appeared as a broad band with the equivalent Bragg's angle at 2θ = 22°, which also indicated the presence of porous silica materials. The maximum intensity observed for silver at (111) plane showed that AgNPs are more oriented in its pore [35].

Results of SEM and TEM of silver, silica and nanohybrid

The Scanning electron microscopy (SEM) and Transmission Electron Microscopy (TEM) micrographs of the surface and internal morphologies of porous silica are shown in Plate 1. The results showed that porous silica particles of sizes below 100 nm were obtained. These primary particles showed a big tendency to aggregate and form larger particle clusters. The micrographs also show that the particles were spherical, which is similar to the findings of Vazquez *et al* [36][29] in a research conducted on 'Synthesis of mesoporous silica nanoparticles by sol–gel as nanocontainer for future drug delivery applications'. Micrographs demonstrated a variety of particle sizes due low concentration of CTAB agglomeration. The SEM micrograph of the surface morphology of silver nanoparticles is shown in Plate 2. Nanorods of silver particles were obtained, these primary particles showed a big tendency to aggregate and form larger particle clusters. The TEM result for silver also revealed that the particles obtained were of rod shapes (Plate 3). Plate 4 shows the core - shell of Ag – SiO_2 nanocomposite with Ag (core) of 73 nm diameter being surrounded by silica (shell) of 12 nm. The formation of core-shell Ag–SiO_2 nanocomposite is shown in plate 3.

ISSN 0795 - 22066

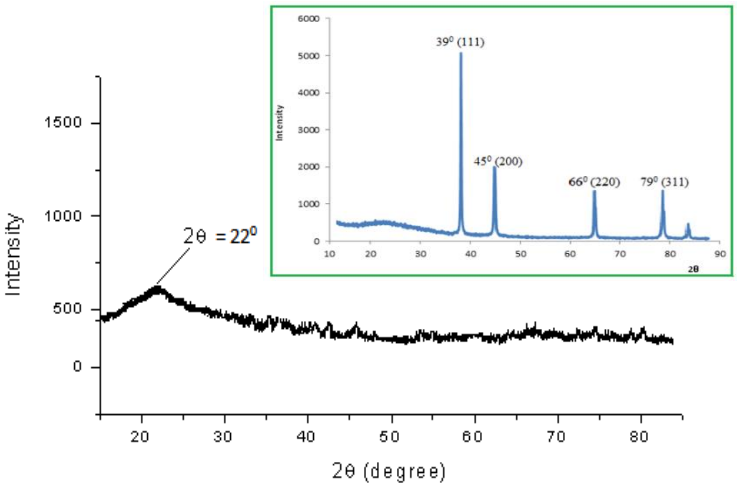

Figure 3 and 4: XRD of porous silica and Ag Nanoparticle (**Fig 4 - Insert**)

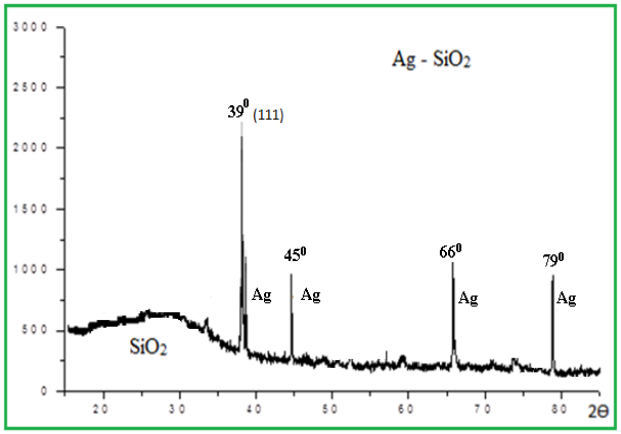

Figure 5: XRD of Ag–SiO_2

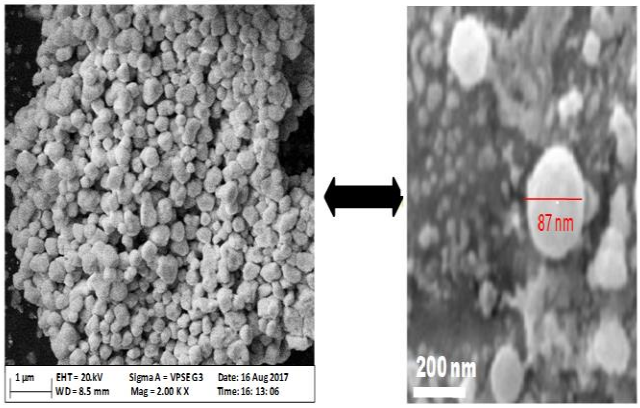

Plate 2: SEM and TEM of porous Silica

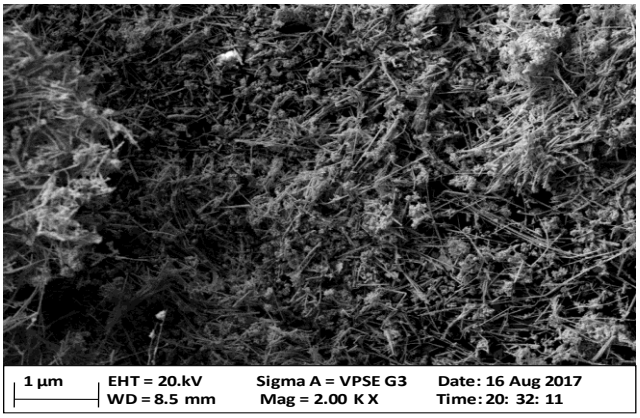

Plate 2: SEM of Silver nanoparticles

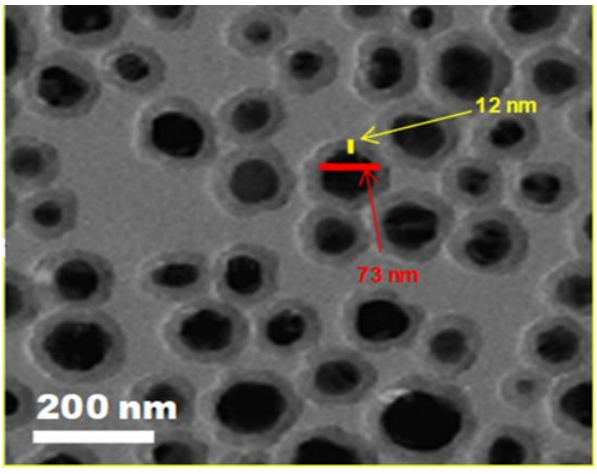

Plate 3: TEM images of silver nanorods

ISSN 0795 - 22066

Results of Energy Dispersed X-Ray Spectroscopy (EDX)

The observed EDX result in Figure 8 shows that the synthesized Ag-SiO_2 contains approximately 83.3 wt % silica (Si and O) and 16.7% silver (1:5) respectively. This result is attributed to the formation of core (Ag) - Shell (SiO_2) nanohybrid unlike the result in the research conducted by Tomer *et al* [19] in which 49.1 - 64% Ag nanoparticles were dispersed in the pores of silica SBA-15 by hydrothermal method. Due to the absence of other elements such as C, Na and Cl or Br, the EDX measurement of Ag–SiO_2 powder shows that the contents (SiO_2 and Ag) were, 99.9 (% in wt%) pure. This finding is in perfect agreement with the result obtained by [37] [38] (Figure 6).

Results of UV visible for Ag–SiO_2 nanocomposite

UV-Visible absorption spectra of different sizes of Ag–SiO_2 nanocomposites showed max at 221 – 228 nm and 421 nm for silica and silver respectively (Figure 7). The peak at 421 nm is the Surface Plasmon Resonance (SPR) absorption peak which is a characteristic peak of silver as well as silver oxide nanoparticles as per the result obtained by Nguyen *et al* [39]. Metal nanoparticles have free electrons, which yield a surface Plasmon resonance (SPR) absorption band, due to the mutual vibration of electrons of metal nanoparticles in resonance with light wave [21]. The optical properties of the nanoparticles strongly influence their sensing properties. The absorption intensity of nano-hybrid Ag-SiO_2 slightly red shifted to the visible region (Figure 9). This can be attributed to the charge transition between the surface silver and silica, which can promote sensing responses. The optical band gaps were found to be 3.12 - 4.11 eV for silica and silver respectively, which is closely related to the range of 3.65 - 3.47 eV observed by [40] [41].

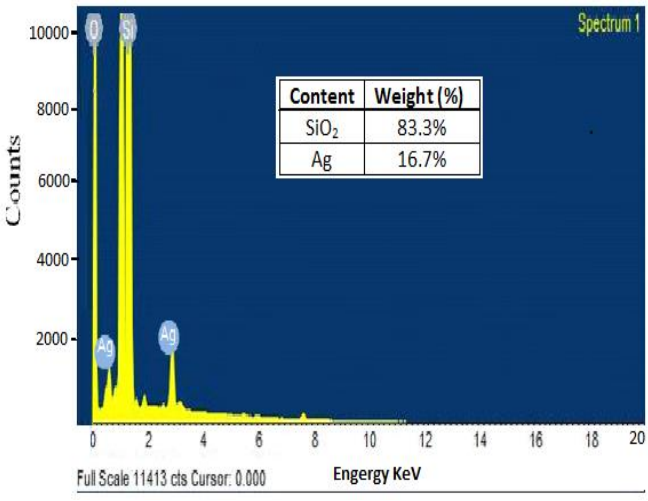

Figure 6: EDX of Ag-SiO_2

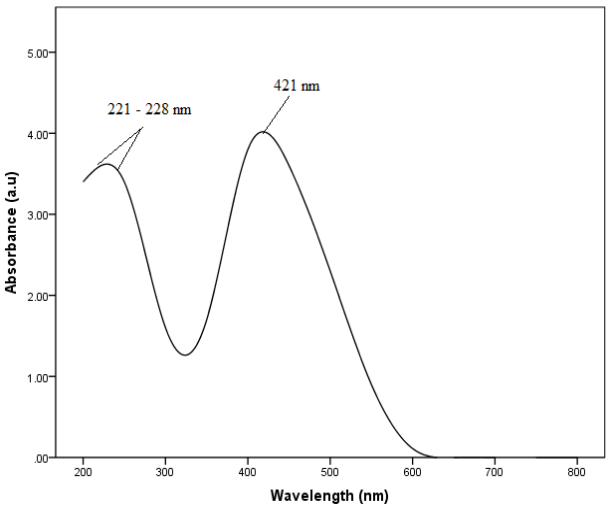

Figure 7: UV-Visible spectrum of Ag-SiO_2 nanocomposite

ISSN 0795 - 22066

Pore size and pore volume of Ag-SiO_2

Porosity is typically defined as a ratio of pore volume to the total volume of the particle. The pore size distribution of the silica network was measured by the N_2 adsorption–desorption measurements. As shown in Figure 8, there were small pores with a broad distribution from 3 – 8 nm. The curve shows that most of the pores were within a size smaller than 8 nm. The probability pore size estimated from the peak position was about 6 nm, which is an indication that the nanocomposite possessed a relatively narrow pore size distribution for adequate adsorption of water molecules. The average pore size of 6 nm got from this study is smaller than the average pore size of 8.5 nm obtained by Tomer *et al* [19] [42].

Results of X-ray Photoelectron Spectroscopy (XPS)

Figures 9 and 10 show the core level spectra recorded from Ag–SiO_2 where Ag is the core and SiO_2 is the shell. Ag 3d core level could be decomposed into two chemically distinct species ($3d_{3/2}$ and $3d_{5/2}$) that are assigned to metallic silver and few unreacted silver ion.These peaks signify that Ag metal predominantly is in its zerovalent state. The metallic Ag 3d peaks were centered at approximately 368 and 374 eV (Figure 9) as per 366.35 and 368.5 eV observed by Peszke *et al* [43] while Figure 12 shows the O (1s) spectrum peak centred on 531.1 eV. The contribution to the peak originates from O^{2-} in the SiO_2 lattice. The positions of these peaks are in agreement with published data [30, 31]. There may be a contribution from loosely bond oxygen on the structure of SiO_2 nanocrystals O^{2-} ion in the oxygen deficient regions. The relatively low Ag 3d binding energy peak position (368 eV) compared with a higher binding energy for SiO_2 (533.1 eV) is in good agreement with the data reported for TiO_2 [32, 16, 30] [46].

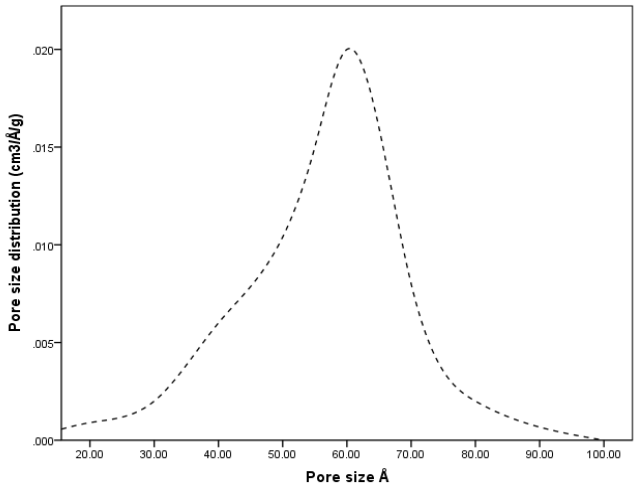

Figure 8: Pore size and pore volume of Ag-SiO

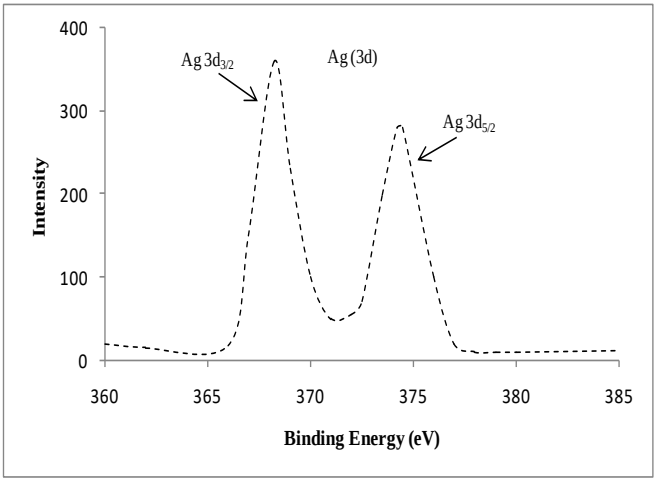

Figure 9: XPS showing binding energy of Silver

ISSN 0795 - 22066

CONCLUSION

Ag-SiO_2 Materials were characterized using various microscopic and spectroscopic techniques. The heterostructured properties of Core-shell silver-silica nanocomposite was elucidated and confirmed by XRD, SEM, UV-visible spectroscopy and N_2 adsorption isotherm. The synthesized silver-silica nanocomposite can further be used as a multifunctional sensing material for agricultural applications, humidity sensor in health and telecommunication facilities. in addition to its promising antimicrobial possibility.

ACKNOWLEDGEMENT

This work was funded by 2019 & 2021 (Merged) TETFUND Institution Based Research Grant (FUNAAB-IBR-01-2022). The authors wish to thank the staff of Chemistry Department and Universities of Western Cape and University of Vender, South Africa and for their supports on bench works and morphological characterization. Our original work in this field was carried out in the postgraduate research laboratories of the Department of Chemistry, FUNAAB. We are grateful to the Management of Federal University of Agriculture, Abeokuta (FUNAAB) for the administrative support towards the securement of the IBR research grant.

REFERENCES

[1] R. Roy, R. A. Roy, and D. M. Roy, "Alternative perspectives on 'quasicrystallinity': non-uniformity and nanocomposites," *Mater. Lett.*, vol. 4, no. 8–9, pp. 323–328, 1986, doi: doi.org/10.1016/0167-577X(86)90063-7.

[2] D. Schmidt, D. Shah, and E. P. Giannelis, "New advances in polymer/layered silicate nanocomposites," *Curr. Opin. Solid State Mater. Sci.*, vol. 6, no. 3, pp. 205–212, 2002, doi: 10.1016/S1359-0286(02)00049-9.

[3] H. Gleiter, "Nanostructured Materials: Basic Concepts And Microstructure p." [Online]. Available: www.elsevier.com/locate/actamat

[4] O. Kamigaito, "What can be improved by nanometer composites? Journal of the Japan Society of Powder and Powder Metallurgy, 38(3), 315–321.," vol. 38, no. 3, pp. 315–321, 1991, doi: 10.2497/jjspm.38.315.

[5] S. S. Ray, K. Yamada, M. Okamoto, and K. Ueda, "Polylactide-Layered Silicate Nanocomposite: A Novel Biodegradable Material," *Nano Lett.*, vol. 2, no. 10, pp. 1093–1096, 2002, doi: 10.1021/nl0202152.

[6] J. Ou, M. Huang, Y. Wu, S. Huang, J. Lu, and S. Wu, "Additive manufacturing of flexible polymer-derived ceramic matrix composites," *Virtual Phys. Prototyp.*, vol. 18, no. 1, 2023, doi: 10.1080/17452759.2022.2150230.

[7] S. C. Tjong and G. S. Wang, "High-cycle fatigue properties of Al-based composites reinforced with in situ TiB2 and Al2O3 particulates," *Mater. Sci. Eng. A*, vol. 386, no. 1–2, pp. 48–53, 2004, doi: 10.1016/j.msea.2004.07.021.

[8] H. Fischer, "Polymer nanocomposites: From fundamental research to specific applications," *Mater. Sci. Eng. C*, vol. 23, no. 6–8, pp. 763–772, Dec. 2003, doi: 10.1016/j.msec.2003.09.148.

[9] X. K. Meng, S. C. Tang, and S. Vongehr, "A Review on Diverse Silver Nanostructures," *J. Mater. Sci. Technol.*, vol. 26, no. 6, pp. 487–522, 2010, doi: 10.1016/S1005-0302(10)60078-3.

[10] A. K. Kheirabad, S. Zhou, Y. Lu, and G.

ISSN 0795 - 22066

Mcinerney, "Colloidal dispersion of poly (ionic liquid)/ Cu composite particles for protective surface coating against SAR-CoV-2," no. February 2021, pp. 227–232, 2022, doi: 10.1002/nano.202100069.

[11] A. K. Mittal, Y. Chisti, and U. C. Banerjee, "Synthesis of metallic nanoparticles using plant extracts," *Biotechnol. Adv.*, vol. 31, no. 2, pp. 346–356, 2013, doi: 10.1016/j.biotechadv.2013.01.003.

[12] W. Zhang, X. Qiao, and J. Chen, "Synthesis of silver nanoparticles-Effects of concerned parameters in water/oil microemulsion," *Mater. Sci. Eng. B Solid-State Mater. Adv. Technol.*, vol. 142, no. 1, pp. 1–15, 2007, doi: 10.1016/j.mseb.2007.06.014.

[13] B. Dong *et al.*, "Ultrasonics Sonochemistry Synthesis of monodisperse spherical AgNPs by ultrasound-intensified Lee-Meisel method , and quick evaluation via machine learning," vol. 73, 2021.

[14] A. Heuer-jungemann *et al.*, "The Role of Ligands in the Chemical Synthesis and Applications of Inorganic Nanoparticles," *Chem. Rev.*, 2018, doi: 10.1021/acs.chemrev.8b00733.

[15] A. Henglein and M. Giersig, "Formation of Colloidal Silver Nanoparticles: Capping Action of Citrate.," *J. Phys. Chem. B*, vol. 46556, no. 2, pp. 9533–9539, 1999, [Online]. Available: http://pubs.acs.org/doi/abs/10.1021/jp9925334

[16] and M. A. Z. serenella medici, Massimiliano Francesco Peana, Valeria Marina Nurchi, "The medical uses of silver : history , myths and scientific evidence," 2019, doi: 10.1021/acs.jmedchem.8b01439.

[17] A. Luceri, R. Francese, D. Lembo, M. Ferraris, and C. Balagna, "Silver Nanoparticles: Review of Antiviral Properties, Mechanism of Action and Applications," *Microorganisms*, vol. 11, no. 3, p. 629, 2023, doi: 10.3390/microorganisms11030629.

[18] A. A. Antsiferova, P. K. Kashkarov, and M. V. Koval'chuk, "Effect of Different Forms of Silver on Biological Objects," *Nanobiotechnology Reports*, vol. 17, no. 2, pp. 155–164, 2022, doi: 10.1134/S2635167622020021.

[19] T. Watcharatharapong *et al.*, "Effect of Transition Metal Cations on Stability Enhancement for Molybdate-Based Hybrid Supercapacitor," *ACS Appl. Mater. Interfaces*, vol. 9, no. 21, pp. 17977–17991, 2017, doi: 10.1021/acsami.7b03836.

[20] S. Salnus *et al.*, "1129 Review : A Review on Green Synthesis , Antimicrobial Applications and Toxicity of Silver Nanoparticles Mediated by Plant Extract," vol. 22, no. 4, pp. 1129–1143, 2022, doi: 10.22146/ijc.71053.

[21] N. Bano *et al.*, "Antibacterial efficacy of synthesized silver nanoparticles of Microbacterium proteolyticum LA2 (R) and Streptomyces rochei LA2 (O) against biofilm forming meningitis causing microbes," *Sci. Rep.*, pp. 1–14, 2023, doi: 10.1038/s41598-023-30215-9.

[22] R. Kanthasamy and S. C. Larsen, "Visible light photoreduction of Cr(VI) in aqueous solution using iron-containing zeolite tubes," *Microporous Mesoporous Mater.*, vol. 100, no. 1–3, pp. 340–349, 2007, doi: 10.1016/j.micromeso.2006.11.021.

[23] W. Song, R. E. Justice, C. A. Jones, V. H. Grassian, and S. C. Larsen, "Size-dependent properties of nanocrystalline silicalite synthesized with systematically varied crystal sizes," *Langmuir*, vol. 20, no. 11, pp. 4696–4702, 2004, doi: 10.1021/la049817m.

[24] Q. F. Zhou, J. C. Bao, and Z. Xu, "Shape-controlled synthesis of nanostructured gold by a protection-reduction technique," *J. Mater. Chem.*, vol. 12, no. 2, pp. 384–387, 2002, doi: 10.1039/b103767f.

ISSN 0795 - 22066

[25] A. Lázaro García, *Nano-silica production at low temperatures from the dissolution of olivine, PhD Thesis,*.

[26] I. A. Rahman and V. Padavettan, "Synthesis of Silica nanoparticles by Sol-Gel: Size-dependent properties, surface modification, and applications in silica-polymer nanocompositesa review," *J. Nanomater.*, vol. 2012, 2012, doi: 10.1155/2012/132424.

[27] Z. Rahimabadi, "Synthesis , characterization , and the study of structural and optical properties of core / shell nanoparticles of SiO 2 @ CuO for solar absorption collectors application," *J. Mater. Sci. Mater. Electron.*, 2022, doi: 10.1007/s10854-022-07928-0.

[28] V. K. Tomer *et al.*, "Corrigendum to: Humidity-Sensing Properties of Ag 0 Nanoparticles Supported on WO 3 -SiO 2 with Super Rapid Response and Excellent Stability : Rapid and Stable Humidity Sensing (European Journal of Inorganic Chemistry, (2015), 2015, 31, (5232-5240), 10.10," *Eur. J. Inorg. Chem.*, vol. 2019, no. 45, p. 4862, 2019, doi: 10.1002/ejic.201901156.

[29] Z. Alam, S. Ghamami, and S. Baghshahi, "Synthesis and characterization of hollow mesoporous silica nanocomposites containing phosphorescent pigment and doxycycline," *Nano Sel.*, vol. 4, no. 3, pp. 192–201, 2023, doi: 10.1002/nano.202200216.

[30] M. G. V. V Gowthami and A. Sahoo, "Preparation and characterization of amorphous silica and metal modified silica catalyst from rice husk Chemical Engineering."

[31] K. Anandalakshmi, J. Venugobal, and V. Ramasamy, "Characterization of silver nanoparticles by green synthesis method using Pedalium murex leaf extract and their antibacterial activity," *Appl. Nanosci.*, vol. 6, no. 3, pp. 399–408, 2016, doi: 10.1007/s13204-015-0449-z.

[32] K. Jyoti, M. Baunthiyal, and A. Singh, "Characterization of silver nanoparticles synthesized using Urtica dioica Linn. leaves and their synergistic effects with antibiotics," *J. Radiat. Res. Appl. Sci.*, vol. 9, no. 3, pp. 217–227, Jul. 2016, doi: 10.1016/j.jrras.2015.10.002.

[33] S. P. Dubey, M. Lahtinen, and M. Sillanpää, "Tansy fruit mediated greener synthesis of silver and gold nanoparticles," *Process Biochem.*, vol. 45, no. 7, pp. 1065–1071, Jul. 2010, doi: 10.1016/j.procbio.2010.03.024.

[34] K. J. Wu, E. C. M. Tse, C. Shang, and Z. Guo, "Nucleation and growth in solution synthesis of nanostructures – From fundamentals to advanced applications," *Prog. Mater. Sci.*, vol. 123, no. May, pp. 1–45, 2022, doi: 10.1016/j.pmatsci.2021.100821.

[35] D. Acharya and B. Mohanta, "Optical properties of synthesized Ag and Ag@SiO2 core-shell nanoparticles," in *AIP Conference Proceedings*, American Institute of Physics Inc., May 2017. doi: 10.1063/1.4980388.

[36] N. I. Vazquez, Z. Gonzalez, B. Ferrari, and Y. Castro, "Synthesis of mesoporous silica nanoparticles by sol-gel as nanocontainer for future drug delivery applications," *Bol. la Soc. Esp. Ceram. y Vidr.*, vol. 56, no. 3, pp. 139–145, 2017, doi: 10.1016/j.bsecv.2017.03.002.

[37] A. R. Maurice and H. Faouzi, "Synthesis and Characterization of Amorphous Silica Nanoparitcles from Aqueous Silicates Uisng Cationic Surfactants," *J. Met. Mater. Miner.*, vol. 24, no. 1, pp. 37–42, 2014.

[38] E. Al-Bermany, A. T. Mekhalif, H. A. Banimuslem, K. Abdali, and M. M. Sabri, "Effect of green synthesis bimetallic Ag@SiO2 core–shell nanoparticles on absorption behavior and electrical properties of PVA-PEO nanocomposites for optoelectronic applications," *Silicon*, no. 0123456789, 2023, doi:

ISSN 0795 - 22066

10.1007/s12633-023-02332-7.

[39] H. C. Nguyen, T. T. Nguyen, T. H. Dao, Q. B. Ngo, H. L. Pham, and T. B. N. Nguyen, "Preparation of Ag/SiO2 nanocomposite and assessment of its antifungal effect on soybean plant (a Vietnamese species DT-26)," *Adv. Nat. Sci. Nanosci. Nanotechnol.*, vol. 7, no. 4, Dec. 2016, doi: 10.1088/2043-6262/7/4/045014.

[40] V. K. Tomer and S. Duhan, "Nano titania loaded mesoporous silica: Preparation and application as high performance humidity sensor," *Sensors Actuators, B Chem.*, vol. 220, pp. 192–200, 2015, doi: 10.1016/j.snb.2015.05.072.

[41] T. T. T. Bui *et al.*, "Study of stability and antimicrobial activity of colloidal Ag/SiO2nanocomposites," *Adv. Nat. Sci. Nanosci. Nanotechnol.*, vol. 12, no. 2, p. 25010, 2021, doi: 10.1088/2043-6262/ac079c.

[42] S. Cheng, T. Meng, D. Mao, X. Guo, and J. Yu, "Ni-Modified Ag/SiO2 Catalysts for Selective Hydrogenation of Dimethyl Oxalate to Methyl Glycolate Shuai," *ACS Omega*, vol. 7, no. 45, pp. 41224–41235, 2022, doi: 10.1021/acsomega.2c04880.

[43] J. Peszke *et al.*, "Unique properties of silver and copper silica-based nanocomposites as antimicrobial agents," *RSC Adv.*, vol. 7, no. 45, pp. 28092–28104, 2017, doi: 10.1039/c7ra00720e.

[44] V. G. Pol *et al.*, "Sonochemical deposition of silver nanoparticles on silica spheres," *Langmuir*, vol. 18, no. 8, pp. 3352–3357, Apr. 2002, doi: 10.1021/la0155552.

[45] J. Schnadt *et al.*, "Structural study of adsorption of isonicotinic acid and related molecules on rutile TiO2(1 1 0) II: XPS," *Surf. Sci.*, vol. 544, no. 1, pp. 74–86, 2003, doi: 10.1016/j.susc.2003.08.013.

[46] P. Prepelita, F. Garoi, M. Dumitru, and V. Craciun, "Implementation of Ag/ SiO2 nanofilms for metamaterial engineering," *Results Phys.*, vol. 35, no. February, p. 105387, 2022, doi: 10.1016/j.rinp.2022.105387.

ISSN 0795 - 22066